Published in final edited form as:
Dent Mater. 2014 May ; 30(5): 535–544. doi:10.1016/j.dental.2014.02.007.

Prevascularization of biofunctional calcium phosphate cement for dental and craniofacial repairs

Wenchuan Chen[a,b], **WahWah Thein-Han**[b], **Michael D. Weir**[b], **Qianming Chen**[a], and **Hockin H.K. Xu**[b,c,d,e]

[a] State Key Laboratory of Oral Diseases, West China Hospital of Stomatology, Sichuan University, Chengdu, Sichuan 610041, China

[b] Biomaterials & Tissue Engineering Division, Department of Endodontics, Prosthodontics and Operative Dentistry, University of Maryland Dental School, Baltimore, MD 21201, USA

[c] Center for Stem Cell Biology and Regenerative Medicine, University of Maryland School of Medicine, Baltimore, MD 21201, USA

[d] University of Maryland Marlene and Stewart Greenebaum Cancer Center, University of Maryland School of Medicine, Baltimore, MD 21201, USA

[e] Department of Mechanical Engineering, University of Maryland, Baltimore County, MD 21250, USA

Abstract

Objectives—Calcium phosphate cement (CPC) is promising for dental and craniofacial repairs. Vascularization in bone tissue engineering constructs is currently a major challenge. The objectives of this study were to investigate the prevascularization of macroporous CPC via coculturing human umbilical vein endothelial cells (HUVEC) and human osteoblasts (HOB), and determine the effect of RGD in CPC on microcapillary formation for the first time.

Methods—Macroporous CPC scaffold was prepared using CPC powder, chitosan liquid and gas-foaming porogen. Chitosan was grafted with Arg-Gly-Asp (RGD) to biofunctionalize the CPC. HUVEC and HOB were cocultured on macroporous CPC-RGD and CPC control without RGD for up to 42 d. The osteogenic and angiogenic differentiation, bone matrix mineral synthesis, and formation of microcapillary-like structures were measured.

Results—RGD-grafting in CPC increased the genes expressions of osteogenic and angiogenic differentiation markers than those of CPC control without RGD. Cell-synthesized bone mineral content also increased on CPC-RGD, compared to CPC control ($p < 0.05$). Immunostaining with endothelial marker showed that the amount of microcapillary-like structures on CPC scaffolds

Correspondence: Hockin H. K. Xu, Professor, Director of Biomaterials & Tissue Engineering Division, Department of Endodontics, Prosthodontics and Operative Dentistry, University of Maryland Dental School, 650 West Baltimore Street, Baltimore, MD 21201, USA. Tel.: +1 410 706 7047; fax: +1 410 706 3028; hxu@umaryland.edu..

increased with time. At 42 d, the cumulative vessel length for CPC-RGD scaffold was 1.69-fold that of CPC control. SEM examination confirmed the morphology of self-assembled microcapillary-like structures on CPC scaffolds.

Significance—HUVEC+HOB coculture on macroporous CPC scaffold successfully achieved prevascularization. RGD incorporation in CPC enhanced osteogenic differentiation, bone mineral synthesis, and microcapillary-like structure formation. The novel prevascularized CPC-RGD constructs are promising for dental, craniofacial and orthopedic applications.

Keywords

Macroporous calcium phosphate cement; prevascularization; RGD biofunctionalization; bone regeneration; endothelial cells; osteoblasts

1. Introduction

The need for bone repair in dental, craniofacial and orthopedic applications has increased as the world population ages [1-3]. Tissue engineering approaches are being developed with promising results for regenerative medicine applications [4-8]. The reconstruction of large skeletal defects, however, is still a major orthopedic challenge for tissue engineering strategies due to inadequate vascularization [9]. A slow or incomplete vascularization at the defects where bone biomaterials were implanted *in vivo* would result in inadequate oxygen and nutrition supply and waste products removal, leading to hypoxia and cell death. Therefore, the development of a functional microvasculature and angiogenesis in bone tissue constructs are vital to achieve successful therapeutic outcome in bone regeneration [10]. To achieve rapid and sufficient angiogenesis, several approaches were investigated, including the application of angiogenic growth factors in biomaterials to induce angiogenesis into implants *in vivo* [11-15], and the creation of microvascular networks on biomaterials *in vitro* before implantation (prevascularization) [14-18]. The prevascularization approach may help achieve success if the host vascular system can be integrated with the preformed vasculature to rapidly establish circulation throughout the biomaterial scaffold after implantation.

Calcium phosphate cements are promising for bone repair because of their injectability and biocompatibility [2,5,19-21]. A calcium phosphate cement comprising of a mixture of tetracalcium phosphate [TTCP: $Ca_4(PO_4)_2O$] and dicalcium phosphate anhydrous (DCPA: $CaHPO_4$) was referred to as CPC [19,22]. Due to its excellent osteoconductivity and bone replacement capability, CPC was approved in 1996 by the Food and Drug Administration for repairing craniofacial defects in humans, thus becoming the first CPC available for clinical use [19]. CPC can be molded to the desired shape for esthetics and set to form a scaffold for bone ingrowth. Potential dental and craniofacial applications of CPC include mandibular and maxillary ridge augmentation, periodontal bone repair, support of metal dental implants or augmentation of deficient implant sites, and major reconstructions of the maxilla or mandible after trauma or tumor resection. However, limited angiogenesis and insufficient bone formation was observed with calcium phosphate biomaterials [11]. Angiogenic growth factors have been used to address this issue [11]. Another promising approach to overcome this problem is *in vitro* prevascularization of the scaffold [14,15]. This can potentially be achieved via the coculture of endothelial cells and osteoprogenitor

cells [16-18]. A previous study cocultured endothelial cells and osteoblasts on porous hydroxyapatite, porous β-tricalcium phosphate, porous nickel-titanium, and silk fibroin nets, yielding a tissue-like self-assembly of cells with endothelial cells forming microcapillary-like structures [16]. Another study used starch-based scaffold to coculture osteoblasts and endothelial cells and obtained microcapillary-like structures [17]. However, a literature search revealed no report on prevascularization of CPC, except our recent study on coculture of endothelial cells and osteoblasts on CPC without biofunctionalization [23], in which cell attachment was not robust.

Therefore, the aim of the present study was to investigate the prevascularization of CPC by coculture of human umbilical vein endothelial cells (HUVEC) and human osteoblasts (HOB) on a biofunctionalized CPC scaffold. RGD was grafted with chitosan which was then mixed into CPC to yield a CPC-RGD scaffold to enhance cell attachment and function, which was compared to CPC control without RGD. A gas-foaming method was used to create macropores in CPC. It was hypothesized that: (1) CPC-RGD scaffold seeded with HUVEC and HOB will have higher angiogenic and osteogenic gene expressions than CPC control; (2) CPC-RGD scaffold seeded with HUVEC and HOB will have more bone mineral synthesis than CPC control; (3) CPC-RGD scaffold seeded with HUVEC and HOB will generate much more microcapillary-like structures than CPC control.

2. Materials and methods

2.1. Fabrication of gas-foaming CPC with immobilized adhesive peptide

CPC powder consisted of an equimolar mixture of TTCP and DCPA. TTCP was synthesized from a solid-state reaction between $CaHPO_4$ and $CaCO_3$ (J. T. Baker, Phillipsburg, NJ) and then ground to obtain a median particle size of 17 μm. The DCPA powder was ground to obtain a median particle size of 1 μm. The TTCP and DCPA powders were mixed in a blender to form the CPC powder with a TTCP:DCPA molar ratio of 1:1. CPC liquid consisted of chitosan malate (Vanson, Redmond, WA) mixed with distilled water at a chitosan/(chitosan + water) mass fraction of 15%. Chitosan was used because it could cause fast-setting to CPC paste and strengthen the CPC [24]. RGD was immobilized with chitosan by coupling G4RGDSP (Thermo Fisher, Waltham, MA) with chitosan. This was achieved by forming amide bonds between carboxyl groups in peptide and residual amine groups in chitosan, using 1-Ethyl-3-[3-dimethylaminopropyl] carbodiimide hydrochloride (EDC, Thermo Fisher) and sulfo-*N*-hydroxysuccinimide (Sulfo-NHS, Thermo Fisher) as coupling agents [25-27]. After dissolving G4RGDSP peptide (12.4 mg, 16.32×10^{-6} mol) in 0.1 mol/L of 2-(N-Morpholino) ethanesulfonic acid (MES) buffer (4 mL) (Thermo Fisher), EDC (3.76 mg, 19.6×10^{-6} mol) and Sulfo-NHS (0.28 mg, 2.44×10^{-6} mol) were added to the peptide solution (molar ratio of G4RGDSP:EDC:NHS = 1:1.2:0.6). The solution was incubated at room temperature for 30 min to activate the terminal carboxyl group of proline. Then, this solution was added to the chitosan solution dissolved in 0.1 mol/L of MES buffer (100 mL, 1 wt%). The coupling reaction was performed for 24 h at room temperature [25-27]. The products were dialyzed against distilled water using a Dialysis Cassettes (MWCO = 3.5 kDa) (Thermo Fisher) for 3 days to remove the uncoupled peptides by

changing water 3 times daily. Finally, the products were freeze-dried to yield RGD-immobilized chitosan [25-27].

A gas-foaming method was used to create macropores in CPC. Following a previous study [28], sodium bicarbonate ($NaHCO_3$) and citric acid monohydrate ($C_6H_8O_7{\cdot}H_2O$) were added into CPC as the porogen. The acid-base reaction of $C_6H_8O_7{\cdot}H_2O$ with $NaHCO_3$ produced CO_2 bubbles in CPC, resulting in macropores [29]. $NaHCO_3$ was added to the CPC powder at a $NaHCO_3/(NaHCO_3$ + CPC powder) mass fraction of 15%. The corresponding amount of $C_6H_8O_7{\cdot}H_2O$ was added to the CPC liquid, to maintain a $NaHCO_3/(NaHCO_3 + C_6H_8O_7{\cdot}H_2O)$ mass fraction of 54.52%, following a previous study [28].

CPC paste was formed by mixing CPC powder with CPC liquid at a powder to liquid mass ratio of 2 to 1. The paste was placed in Teflon molds to fabricate macroporous CPC disks with 12 mm in diameter and 1.5 mm in thickness. Two types of materials were fabricated: CPC control (in which the cement liquid used chitosan without RGD), and CPC-RGD (using chitosan with RGD). Specimens were set in a humidor with 100% relative humidity for 24 h at 37°C, sterilized in an ethylene oxide sterilizer (Andersen, Haw River, NC) for 12 h and then degassed for 7 d prior to cell seeding.

2.2. Cell cultures

HUVEC (Lonza, Walkersville, MD) were cultured in Endothelial Cell Growth Medium-2 (EGM-2; Lonza) which consisted of Endothelial Cells Basal Medium-2 (EBM-2; Lonza) and a provided kit (Lonza). HOB (Lonza) were cultured in Osteoblast Growth Medium (OGM; Lonza) which consisted of Osbteoblasts Basal Medium (OBM; Lonza) and a provided kit (Lonza). Fourth passages of cells were used for the study. At 80% to 90% confluence, cells were detached by trypsin-EDTA (Invitrogen, Carlsbad, CA) and washed twice with phosphate-buffered saline (PBS). HUVEC were mixed with HOB at 4:1 ratio in EGM-2 for coculture [17]. The macroporous CPC disks were pre-incubated with EGM-2 for 3 h in a humidified incubator prior to cell seeding. Then, they were placed individually in 12-well petri plate. The mixed HUVEC + HOB suspension (1.5×10^5 cells/disk) was seeded drop-wise on the top surface of each disk and cultured with EGM-2 in a humidified incubator (5% CO_2, 37 °C) for up to 42 d. The medium was replaced every 2 d.

2.3. Quantitative real time-PCR

Quantitative real-time polymerase chain reaction (qRT-PCR, 7900HT, Applied Biosystems, Foster City, CA) was used to measure gene expression of cells on CPC at 14 d, 28 d, and 42 d. The total cellular RNA of the cells was extracted with TRIzol reagent (Invitrogen). RNA concentration was measured via a NanoDrop 2000 spectrophotometer (Thermo Fisher, Wilmington, DE) and diluted to 100 ng/μL if necessary. RNA was reverse-transcribed into cDNA using a High-Capacity cDNA Reverse Transcription kit (Applied Biosystems). TaqMan gene expression assay kits (Applied Biosystems) were used to measure the transcript levels of the following genes: human alkaline phosphatase (ALP, Hs00758162_m1), osteocalcin (OC, Hs00609452_g1), collagen type I (Coll I, Hs00164004), vascular endothelial growth factor A (VEGF, HS00900055_ml), von-Willebrand factor

(vWF, Hs00169795_m1), vascular endothelial cadherin (VE-cadherin, Hs00170986_m1), and glyceraldehyde 3-phosphate dehydrogenase (GAPDH, Hs99999905). Relative expression level for each target gene was evaluated using the $2^{-\Delta\Delta Ct}$ method [30]. The C_t values of target genes were normalized by the C_t of the TaqMan human housekeeping gene GAPDH to obtain the ΔC_t values. The C_t of HUVEC + HOB cocultured on tissue culture polystyrene for 1 d served as the calibrator.

2.4. Mineral synthesis by cocultured cells

The osteogenesis ability of cocultured cells on the scaffolds was evaluated by staining the minerals synthesized by the cells after 42 d of culture. The CPC disks with cells were washed with PBS, fixed with 10% formaldehyde, and stained with Alizarin Red S (ARS) (Millipore, Billerica, MA) for 20 min, which stained calcium-rich deposits by cells into a red color [31]. An Osteogenesis Kit (Millipore) was used to extract the stained minerals and measure the ARS concentration, following the manufacturer's protocol [27]. An ARS standard curve was established with known concentrations of the dye. CPC control scaffolds with the same compositions and treatments, but without cell seeding, were also measured. The control's ARS concentration was subtracted from the ARS concentration of the cell-seeded scaffolds, to yield the net mineral concentration synthesized by the cells [27,31].

2.5. Immunofluorescent staining of PECAM -1 (CD31)

To determine vascular development, cell-scaffold constructs were immunofluorescent stained for PECAM-1 (CD31, endothelial-specific) (Invitrogen) at 14 d, 28 d, and 42 d. The samples were briefly rinsed twice with PBS, fixed with 4% parformaldehyde for 20 min, washed twice with PBS, permeabilized with 0.5% Triton X-100 for 5 min and blocked with 0.1% bovine serum albumin (BSA) for 30 min. After washing twice with PBS, the samples were incubated with the primary mouse monoclonal antibody anti-human CD31 (1:200, Invitrogen) overnight at 4 °C. The samples were then washed twice with PBS and incubated with secondary antibody (1:1000, goat anti-mouse Alexa Fluor 488, green fluorescence, Invitrogen) for 1 h. This was followed by a brief rinse in PBS, staining of nuclei with DAPI (1 μg/ml, Sigma, St. Louis, MO) for 10 min at room temperature and washing with PBS. The samples were placed in Fluoromount Aqueous Mounting Medium (Sigma) and viewed under epifluorescent microscopy (TE2000S, Nikon, Melville, NY). The capillaries were stained green and showed as tube-like structures. Three random fields of view were imaged from each sample (five samples yielded 15 photos for each time point). The length of capillaries was measured and added together to obtain the cumulative length of capillaries for each image using Image-Pro Plus software (Media Cybernetics, Silver Springs, MD). The cumulative length of capillaries of the image was then divided by the area of that image, to yield the cumulative vessel length per scaffold surface area.

2.6. Scanning electron microscopy of cells on CPC

The cell-scaffold constructs were examined under scanning electron microscopy (SEM, Quanta 200, FEI, Hillsboro, OR, SEM). After culturing for 14 d, the samples were fixed with 2% glutaraldehyde in 0.1 M cacodylate buffer pH 7.4, dehydrated with gradient ethanol, and rinsed with hexamethyldisilazane. The samples were dried overnight, sputter-coated with gold and then examined in SEM.

2.7. Statistical analysis

One-way and two-way ANOVA were performed to detect significant effects of the variables. Tukey's multiple comparison was performed at $p = 0.05$ to analyze the measured values.

3. Results

RT-PCR showed elevated osteogenic and angiogenic differentiation markers, compared to the 1 d expressions of cocultured cells on tissue culture polystyrene which had the value of 1 (Fig. 1). HUVEC+HOB on CPC control and CPC-RGD showed osteogenic differentiation, manifested by ALP, OC and COL I exhibiting high peaks (Fig. 1A-C), where the highest peak in each plot was much higher than 1. For each marker, CPC-RGD had higher peaks than CPC control ($p < 0.05$). These data demonstrate that RGD increased the osteogenic gene expressions of HUVEC+HOB in CPC. The measured angiogenic differentiation genes included VEGF, vWF and VE-cadherin (Fig. 1D-F). In CPC-RGD, up-regulated VEGF expression was 4 times higher than that in CPC control at 14 d ($p < 0.05$). Both in CPC control and CPC-RGD, the vWF gradually decreased from 14 d to 42 d ($p < 0.05$), and the extent of decrease was greater in CPC-RGD than CPC control ($p < 0.05$). VE-cadherin expressions at 28 d and 42 d were higher on CPC-RGD than CPC control ($p < 0.05$).

ARS staining at 42 d revealed a thick and dense red staining of cell mineralization, with a layer of new mineral matrix synthesized by the cells covering the scaffold (Fig. 2A and 2B for CPC control and CPC-RGD, respectively). ARS staining showed a bright red color for CPC without cells because CPC consisted of hydroxyapatite minerals. ARS staining for cell-synthesized matrix showed a darker red color with granular-like morphologies of bone nodule deposits. Cells on CPC-RGD synthesized significantly more ($p < 0.05$) mineral amount than CPC control at each time point (mean ± sd; $n = 5$) (Fig. 2C). Cell-synthesized mineral amount increased with time for both scaffolds ($p < 0.05$). These results indicate that HOB seeded with HUVEC on CPC successfully underwent osteogenic differentiation and mineralization, and RGD incorporation in CPC promoted these processes.

Immunofluorescent staining images of HUVEC + HOB coculture on macroporous CPC control and CPC-RGD are shown in Fig. 3. HUVEC were stained green with endothelial marker PECAM1 on the cell membrane, while cell nuclei were stained blue with DAPI. HOB were only stained blue with DAPI in the nuclei but not green on the cell membrane. Epifluorescent microscopy revealed angiogenic response of HUVEC leading to angiogenic tube formation both on CPC control and CPC-RGD at 14 d (Figs. 3A and 3B). However, more HUVEC clumps without HOB and more branch-like structures were observed on CPC-RGD than CPC control. More branch-like structures were observed with increasing time from 14 d to 28 d (Figs. 3C and 3D). At 42 d, microcapillary-like structures were observed on both scaffolds, with CPC-RGD having more microcapillary-like structures (Figs. 3E and 3F). These microcapillary-like structures were organized as self-assembled tissue-like structures. These results indicate that HUVEC and HOB coculture successfully generated self-assembling organization of microcapillary-like structures on CPC scaffolds.

The cumulative microcapillary length per CPC scaffold area increased over time (Fig. 4A). HUVEC and HOB coculture on CPC-RGD formed significantly more microcapillary-like structures at each time point than CPC control ($p < 0.05$). For both types of constructs, the cumulative microcapillary length increased significantly from 28 d to 42 d ($p < 0.05$). The microcapillary-like structures on CPC-RGD at 14 d were examined in SEM (Figs. 4B and 4C). SEM revealed that the surfaces of scaffolds were completely covered by cells, and some cells formed long tube-like microcapillary structures. The diameters of the microcapillary-like structures were approximately 5 to 10 μm.

4. Discussion

CPC is promising for dental and craniofacial applications due to its injectability, moldability, bioactivity and bone replacement capability. There is a need to enhance vasculature formation to improve the cell-CPC construct function for bone tissue engineering. The present study investigated whether a network of microcapillary-like structures could be generated *in vitro* on a novel macroporous CPC for bone tissue engineering and how vascularization could be enhanced by the addition of RGD. The HUVEC and HOB coculture method was successful in generating microcapillary-like networks on CPC. CPC-RGD was shown to yield higher osteogenic and angiogenic gene expressions, more bone mineral synthesis and more microcapillary-like structures than CPC control. These results indicate that HUVEC and HOB coculture with macroporous CPC scaffolds is a promising approach for vascularization and bone regeneration. While RGD incorporation in CPC could enhance the formation of microcapillary-like structures by endothelial cells, further animal studies are needed to examine the effects on vessel and bone regeneration *in vivo*.

The success of biomaterials after implantation requires a rapid formation of functional blood vessels. Due to their unique role in angiogenesis, endothelial cells are promising in strategic approaches to accomplish bone vascularization. However, endothelial cells on their own cannot complete vessel maturation, because extracellular matrix and mesenchymal cells also play important roles in angiogenesis [32]. Several studies have shown that there is a cross-talk and functional relationship between endothelial cells and osteoblasts-like cells (such as primary osteoblasts and osteoblastic-cell lines) during osteogenesis [33-36]. Therefore, the coculture of endothelial cells with osteoblasts has been proposed as a strategy for angiogenesis and osteogenesis. Several studies showed that coculturing endothelial cells with osteoblasts-like cells resulted in the formation of microcapillary-like structures similar to those observed *in vivo* [17,18]. Although CPC is promising for bone repair due to its excellent biocompatibility and bone replacement capability, little has been reported on prevascularization of CPC, with only one report on coculturing endothelial cells and osteoblasts to prevascularize CPC [23]. The coculture could promote the self-assembled organization of the microcapillary-like structures. However, that CPC contained no RGD for biofunctionalization, and cell attachment was not robust and formation of microvascular networks was slow. In the present study, the macroporous CPC was biofunctionalized via RGD, which significantly enhanced the bone matrix minerals as well as formation of microcapillary-like structures compared to CPC control without RGD.

RGD in CPC likely improved the functions of both HUVEC and HOB due to its stimulatory effects on both osteogenic and angiogenic differentiation. Cells in both constructs underwent osteogenic differentiation with high expressions of ALP, OC, and COL I. These osteogenic markers play key roles in the osteogenic differentiation of mesenchymal stem cells (MSC) [37]. Their higher expressions in CPC-RGD showed that RGD in CPC was beneficial for osteogenesis. This is in agreement with previous studies using different substrates and different types of cells [38-40]. Among these markers, COL I had a significant up-regulation at 14 d and decreased thereafter (Fig. 2C). This indicates that the coculture of HUVEC +HOB on macroporous CPC triggered COL I expression. COL I could mediate cell adhesion, contribute to the mature osteoblast phenotype, provide template for mineralization, as well as drive endothelial cells migration [41-43]. Therefore, the deposit of an extensive network of collagen in the scaffold provides an essential 3D support for HUVEC to migrate and organize into microcapillary-like structures.

VEGF is a powerful pro-angiogenic factor with well-established actions on endothelial cells [34,44]. The higher VEGF expression in CPC-RGD may contribute to its better formation of microcapillary-like structures. vWF is a large multimeric glycoprotein present in blood plasma and is produced constitutively in endothelium [45]. vWF is required for normal hemostasis, and a decreased expression of vWF increases angiogenesis and vessel formation [46,47]. Therefore, the decreased expression of vWF with increasing time in the present study is consistent with the observed increase in vascularization. The fact that vWF at 42 d was lower on CPC-RGD than CPC control is also consistent with the greater microcapillary-like structure formation on CPC-RGD than CPC control. These results are also consistent with a previous study, which showed that vWF decreased while angiogenesis was taking place on a polycaprolactone scaffold [47]. In addition, VE-cadherin is indispensable for proper vascular morphogenesis and serves the purpose of maintaining the newly-formed vessels [48-50]. Its increased expression with time synchronized with the increase of cumulative vessel length on CPC scaffolds. Furthermore, its higher expressions on CPC-RGD than CPC control indicated that RGD in CPC was beneficial for angiogenesis.

The PECAM-1, also known as cluster of differentiation 31 (CD31), is normally found on the surface of endothelial cells and could be used to watch the distribution of epithelial cells. In the present study, the epithelial cells were shown by the staining of PECAM-1 to form microcapillary-like structure. SEM examination also revealed microcapillary-like structures on CPC, which had diameters of 5 to 10 μm, similar to those of natural microcapillaries *in vivo* [51,52]. The mechanism of the microcapillary-like self-assembly is unclear. However, many growth factors have been produced by endothelial cells or osteoblasts to affect the growth and differentiation of the reciprocal cells [34,53,54]. The attachment of HUVEC on scaffold may also be enhanced by the attachment and spreading of HOB, as well as the extracellular matrix production by these cells [16,53]. Eventually, some HUVEC may migrate within the matrix to form microcapillary-like structures. However, the fact that more microcapillary-like structures were observed on CPC-RGD demonstrates that other factors, in addition to the coculture effect, also contributed to the observed vascularization. In particular, the adhesion, proliferation, spreading and migration of cells are affected by surface chemistry, structure, topography and porosity of biomaterials [55,56]. In the present

study, the multipeptide G4RGDSP was incorporated into chitosan by the amide bonds between carboxyl groups on the peptide and amino groups on the chitosan [27]. The RGD sequence in the G4RGDSP can promote the adhesion of cells through the recognition by the adhesion receptors on the cell membrane. Thus, the affinity between cells and biomaterials could be improved by the incorporation of RGD. The improved adhesion of cells may be beneficial for the matrix production by HOB and migration of HUVEC, which together could result in the formation of more microcapillary-like structures on CPC-RGD, than CPC control without RGD. Further study is needed to investigate the coculture of endothelial cells and osteoblasts with macroporous CPC-RGD scaffold for prevascularization and the regeneration of bone and vasculature in an animal model.

5. Conclusions

This study showed for the first time that macroporous CPC scaffold with RGD incorporation achieved much better prevascularization and osteogenesis via HUVEC and HOB coculture than CPC control without RGD. Biofunctionalizing CPC via RGD increased osteogenic and angiogenic differentiation and bone mineralization by the cells. Immunostaining and SEM examination confirmed the generation of microcapillary-like structures on CPC scaffolds. Biofunctionalizing CPC via RGD increased the cumulative vessel length by 1.69-fold, compared to CPC control without RGD. These findings show the promise of generating a prevascularized network on macroporous CPC-RGD scaffold prior to implantation *in vivo* to enhance vascularization and bone regeneration. Therefore, the novel biofunctionalized macroporous CPC with co-seeding of endothelial and osteoblast cells is promising for bone tissue engineering in dental, craniofacial and orthopedic applications.

Acknowledgments

We thank Drs. Laurence C. Chow, Carl G. Simon and Chongyun Bao for fruitful discussions. This study was supported by NIH R01 DE14190 and R21 DE22625 (HX), National Natural Science Foundation of China 81000455 (WC), and the University of Maryland School of Dentistry.

REFERENCES

1. Mao, JJ.; Vunjak-Novakovic, G.; Mikos, AG.; Atala, A. Translational Approaches in Tissue Engineering and Regenerative Medicine. Artech House; Boston, MA: 2007. Chapters 1-3
2. Bohner M. Design of ceramic-based cements and putties for bone graft substitution. Eur Cell Mater. 2010; 20:1–12. [PubMed: 20574942]
3. Park CH, Rios HF, Jin Q, Sugai JV, Padial-Molina M, Taut AD, et al. Tissue engineering bone-ligament complexes using fiber-guiding scaffolds. Biomaterials. 2012; 33:137–45. [PubMed: 21993234]
4. Mao JJ, Giannobile WV, Helms JA, Hollister SJ, Krebsbach PH, Longaker MT, et al. Craniofacial tissue engineering by stem cells. J Dent Res. 2006; 85:966–79. [PubMed: 17062735]
5. Link DP, van den Dolder J, van den Beucken JJ, Wolke JG, Mikos AG, Jansen JA. Bone response and mechanical strength of rabbit femoral defects filled with injectable CaP cements containing TGF-beta 1 loaded gelatin microparticles. Biomaterials. 2008; 29:675–82. [PubMed: 17996293]
6. Hegen A, Blois A, Tiron CE, Hellesoy M, Micklem DR, Nor JE, et al. Efficient in vivo vascularization of tissue-engineering scaffolds. J Tissue Eng Regen Med. 2011; 5:e52–62. [PubMed: 20865694]

7. Liu J, Wang X, Jin Q, Jin T, Chang S, Zhang Z, et al. The stimulation of adipose-derived stem cell differentiation and mineralization by ordered rod-like fluorapatite coatings. Biomaterials. 2012; 33:5036–46. [PubMed: 22483243]
8. Cavalcanti BN, Zeitlin BD, Nor JE. A hydrogel scaffold that maintains viability and supports differentiation of dental pulp stem cells. Dent Mater. 2013; 29:97–102. [PubMed: 22901827]
9. Klenke FM, Liu Y, Yuan H, Hunziker EB, Siebenrock KA, Hofstetter W. Impact of pore size on the vascularization and osseointegration of ceramic bone substitutes in vivo. J Biomed Mater Res A. 2008; 85:777–86. [PubMed: 17896777]
10. Carano RA, Filvaroff EH. Angiogenesis and bone repair. Drug Discov Today. 2003; 8:980–9. [PubMed: 14643161]
11. Wernike E, Montjovent MO, Liu Y, Wismeijer D, Hunziker EB, Siebenrock KA, et al. VEGF incorporated into calcium phosphate ceramics promotes vascularisation and bone formation in vivo. Eur Cell Mater. 2010; 19:30–40. [PubMed: 20178096]
12. Leach JK, Kaigler D, Wang Z, Krebsbach PH, Mooney DJ. Coating of VEGF-releasing scaffolds with bioactive glass for angiogenesis and bone regeneration. Biomaterials. 2006; 27:3249–55. [PubMed: 16490250]
13. Hosseinkhani H, Hosseinkhani M, Khademhosseini A, Kobayashi H, Tabata Y. Enhanced angiogenesis through controlled release of basic fibroblast growth factor from peptide amphiphile for tissue regeneration. Biomaterials. 2006; 27:5836–44. [PubMed: 16930687]
14. Rouwkema J, Rivron NC, van Blitterswijk CA. Vascularization in tissue engineering. Trends Biotechnol. 2008; 26:434–41. [PubMed: 18585808]
15. Lovett M, Lee K, Edwards A, Kaplan DL. Vascularization strategies for tissue engineering. Tissue Eng Part B Rev. 2009; 15:353–70. [PubMed: 19496677]
16. Unger RE, Sartoris A, Peters K, Motta A, Migliaresi C, Kunkel M, et al. Tissue-like self-assembly in cocultures of endothelial cells and osteoblasts and the formation of microcapillary-like structures on three-dimensional porous biomaterials. Biomaterials. 2007; 28:3965–76. [PubMed: 17582491]
17. Santos MI, Unger RE, Sousa RA, Reis RL, Kirkpatrick CJ. Crosstalk between osteoblasts and endothelial cells co-cultured on a polycaprolactone-starch scaffold and the in vitro development of vascularization. Biomaterials. 2009; 30:4407–15. [PubMed: 19487022]
18. Rouwkema J, de Boer J, Van Blitterswijk CA. Endothelial cells assemble into a 3-dimensional prevascular network in a bone tissue engineering construct. Tissue Eng. 2006; 12:2685–93. [PubMed: 16995802]
19. Friedman CD, Costantino PD, Takagi S, Chow LC. BoneSource hydroxyapatite cement: a novel biomaterial for craniofacial skeletal tissue engineering and reconstruction. J Biomed Mater Res. 1998; 43:428–32. [PubMed: 9855201]
20. Jansen JA, Vehof JW, Ruhe PQ, Kroeze-Deutman H, Kuboki Y, Takita H, et al. Growth factor-loaded scaffolds for bone engineering. J Control Release. 2005; 101:127–36. [PubMed: 15588899]
21. Kasten P, Beyen I, Niemeyer P, Luginbuhl R, Bohner M, Richter W. Porosity and pore size of beta-tricalcium phosphate scaffold can influence protein production and osteogenic differentiation of human mesenchymal stem cells: an in vitro and in vivo study. Acta Biomater. 2008; 4:1904–15. [PubMed: 18571999]
22. Brown, WE.; Chow, LC. A new calcium phosphate water setting cement.. In: Brown, PW., editor. Cements Research Progress. Am Ceram Soc.; Westerville, OH: 1986. p. 352-79.
23. Xu HHK, Thein-Han W. Prevascularization of a gas-foaming macroporous calcium phosphate cement scaffold via co-culture of human umbilical vein endothelial cells and osteoblasts. Tissue Eng Part A. 2013; 19:1675–85. [PubMed: 23470207]
24. Zhao L, Weir MD, Xu HHK. An injectable calcium phosphate-alginate hydrogel-umbilical cord mesenchymal stem cell paste for bone tissue engineering. Biomaterials. 2010; 31:6502–10. [PubMed: 20570346]
25. Park KM, Joung KJ, Park KD, Lee SY, Lee MC. RGD-Conjugated Chitosan-Pluronic Hydrogels as a Cell Supported Scaffold for Articular Cartilage Regeneration. Macromol Res. 2008; 16:517–23.

26. Zhou HZ, Chen WC, Weir MD, Xu HHK. Biofunctionalized calcium phosphate cement to enhance the attachment and osteodifferentiation of stem cells released from fast-degradable alginate-fibrin microbeads. Tissue Eng Part A. 2012; 18:1583–95. [PubMed: 22435653]
27. Chen WC, Zhou HZ, Weir MD, Tang MH, Bao CY, Xu HHK. Human embryonic stem cell-derived mesenchymal stem cell seeding on calcium phosphate cement-chitosan-RGD scaffold for bone repair. Tissue Eng Part A. 2013; 19:915–27. [PubMed: 23092172]
28. Chen WC, Zhou HZ, Tang MH, Weir MD, Bao CY, Xu HHK. Gas-foaming calcium phosphate cement scaffold encapsulating human umbilical cord stem cells. Tissue Eng Part A. 2012; 18:816–27. [PubMed: 22011243]
29. Hesaraki S, Zamanian A, Moztarzadeh F. The influence of the acidic component of the gas-foaming porogen used in preparing an injectable porous calcium phosphate cement on its properties: acetic acid versus citric acid. J Biomed Mater Res B Appl Biomater. 2008; 86:208–16. [PubMed: 18161816]
30. Livak KJ, Schmittgen TD. Analysis of relative gene expression data using real-time quantitative PCR and the 2(-Delta Delta C(T)) Method. Methods. 2001; 25:402–8. [PubMed: 11846609]
31. Chen WC, Zhou HZ, Weir MD, Bao CY, Xu HHK. Umbilical cord stem cells released from alginate-fibrin microbeads inside macroporous and biofunctionalized calcium phosphate cement for bone regeneration. Acta Biomater. 2012; 8:2297–306. [PubMed: 22391411]
32. Koike N, Fukumura D, Gralla O, Au P, Schechner JS, Jain RK. Tissue engineering: creation of long-lasting blood vessels. Nature. 2004; 428:138–9. [PubMed: 15014486]
33. Brandi ML, Collin-Osdoby P. Vascular biology and the skeleton. J Bone Miner Res. 2006; 21:183–92. [PubMed: 16418774]
34. Deckers MM, van Bezooijen RL, van der Horst G, Hoogendam J, van Der Bent C, Papapoulos SE, et al. Bone morphogenetic proteins stimulate angiogenesis through osteoblast-derived vascular endothelial growth factor A. Endocrinology. 2002; 143:1545–53. [PubMed: 11897714]
35. Villars F, Guillotin B, Amedee T, Dutoya S, Bordenave L, Bareille R, et al. Effect of HUVEC on human osteoprogenitor cell differentiation needs heterotypic gap junction communication. Am J Physiol Cell Physiol. 2002; 282:C775–85. [PubMed: 11880266]
36. Villanueva JE, Nimni ME. Promotion of calvarial cell osteogenesis by endothelial cells. J Bone Miner Res. 1990; 5:733–9. [PubMed: 2396500]
37. Kim K, Dean D, Mikos AG, Fisher JP. Effect of Initial Cell Seeding Density on Early Osteogenic Signal Expression of Rat Bone Marrow Stromal Cells Cultured on Cross-Linked Poly(propylene fumarate) Disks. Biomacromolecules. 2009; 10:1810–7. [PubMed: 19469498]
38. Yang F, Williams CG, Wang DA, Lee H, Manson PN, Elisseeff J. The effect of incorporating RGD adhesive peptide in polyethylene glycol diacrylate hydrogel on osteogenesis of bone marrow stromal cells. Biomaterials. 2005; 26:5991–8. [PubMed: 15878198]
39. Morgan AW, Roskov KE, Lin-Gibson S, Kaplan DL, Becker ML, Simon CG Jr. Characterization and optimization of RGD-containing silk blends to support osteoblastic differentiation. Biomaterials. 2008; 29:2556–63. [PubMed: 18325585]
40. Hsiong SX, Boontheekul T, Huebsch N, Mooney DJ. Cyclic arginine-glycine-aspartate peptides enhance three-dimensional stem cell osteogenic differentiation. Tissue Eng Part A. 2009; 15:263–72. [PubMed: 18783323]
41. Heino J. The collagen family members as cell adhesion proteins. Bioessays. 2007; 29:1001–10. [PubMed: 17876790]
42. Pham QP, Kasper FK, Scott BL, Raphael RM, Jansen JA, Mikos AG. The influence of an in vitro generated bone-like extracellular matrix on osteoblastic gene expression of marrow stromal cells. Biomaterials. 2008; 29:2729–39. [PubMed: 18367245]
43. Davis GE, Senger DR. Endothelial extracellular matrix: biosynthesis, remodeling, and functions during vascular morphogenesis and neovessel stabilization. Circ Res. 2005; 97:1093–107. [PubMed: 16306453]
44. Roy H, Bhardwaj S, Yla-Herttuala S. Biology of vascular endothelial growth factors. FEBS Lett. 2006; 580:2879–87. [PubMed: 16631753]
45. Sadler JE. Biochemistry and genetics of von Willebrand factor. Annu Rev Biochem. 1998; 67:395–424. [PubMed: 9759493]

46. Starke RD, Ferraro F, Paschalaki KE, Dryden NH, McKinnon TA, Sutton RE, et al. Endothelial von Willebrand factor regulates angiogenesis. Blood. 2011; 117:1071–80. [PubMed: 21048155]
47. Fuchs S, Ghanaati S, Orth C, Barbeck M, Kolbe M, Hofmann A, et al. Contribution of outgrowth endothelial cells from human peripheral blood on in vivo vascularization of bone tissue engineered constructs based on starch polycaprolactone scaffolds. Biomaterials. 2009; 30:526–34. [PubMed: 18977026]
48. Carmeliet P, Lampugnani MG, Moons L, Breviario F, Compernolle V, Bono F, et al. Targeted deficiency or cytosolic truncation of the VE-cadherin gene in mice impairs VEGF-mediated endothelial survival and angiogenesis. Cell. 1999; 98:147–57. [PubMed: 10428027]
49. Gory-Faure S, Prandini MH, Pointu H, Roullot V, Pignot-Paintrand I, Vernet M, et al. Role of vascular endothelial-cadherin in vascular morphogenesis. Development. 1999; 126:2093–102. [PubMed: 10207135]
50. Crosby CV, Fleming PA, Argraves WS, Corada M, Zanetta L, Dejana E, et al. VE-cadherin is not required for the formation of nascent blood vessels but acts to prevent their disassembly. Blood. 2005; 105:2771–6. [PubMed: 15604224]
51. Eriksson E, Myrhage R. Microvascular dimensions and blood flow in skeletal muscle. Acta Physiol Scand. 1972; 86:211–22. [PubMed: 4118267]
52. Potter RF, Groom AC. Capillary diameter and geometry in cardiac and skeletal muscle studied by means of corrosion casts. Microvasc Res. 1983; 25:68–84. [PubMed: 6835100]
53. Bouletreau PJ, Warren SM, Spector JA, Peled ZM, Gerrets RP, Greenwald JA, et al. Hypoxia and VEGF up-regulate BMP-2 mRNA and protein expression in microvascular endothelial cells: implications for fracture healing. Plast Reconstr Surg. 2002; 109:2384–97. [PubMed: 12045566]
54. von Schroeder HP, Veillette CJ, Payandeh J, Qureshi A, Heersche JN. Endothelin-1 promotes osteoprogenitor proliferation and differentiation in fetal rat calvarial cell cultures. Bone. 2003; 33:673–84. [PubMed: 14555273]
55. Hing KA. Bioceramic Bone Graft Substitutes: Influence of Porosity and Chemistry. Int J Appl Ceram Tec. 2005; 2:184–99.
56. Wan Y, Wang Y, Liu Z, Qu X, Han B, Bei J, et al. Adhesion and proliferation of OCT-1 osteoblast-like cells on micro- and nano-scale topography structured poly(L-lactide). Biomaterials. 2005; 26:4453–9. [PubMed: 15701374]

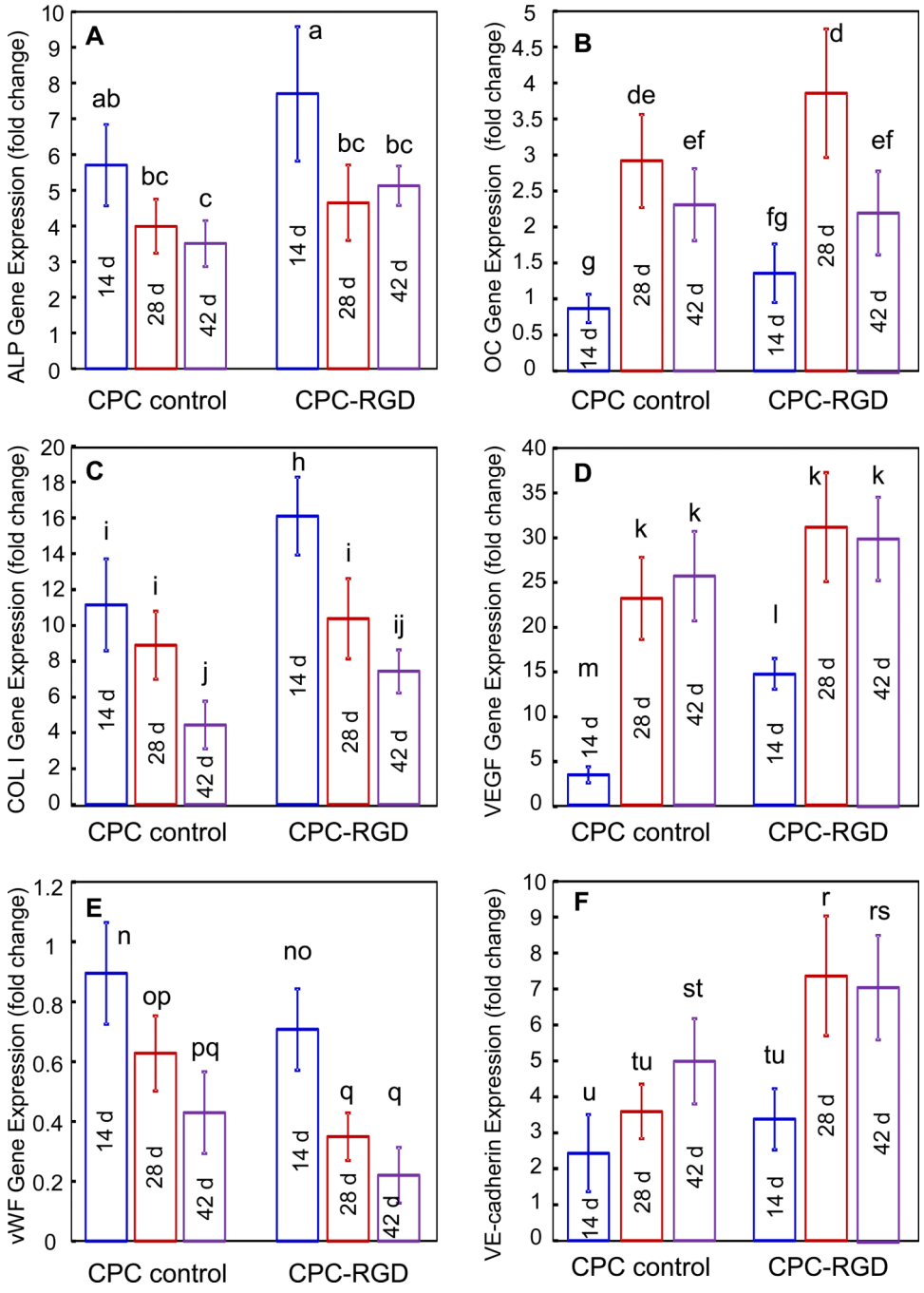

1.

Gene expressions of osteogenic/angiogenic markers of cocultured HUVEC+HOB on CPC scaffolds: (A) ALP; (B) OC; (C) COL I; (D) VEGF; (E) vWF; and (F) VE-cadherin. These expression levels were obtained by real-time PCR at different time points. Bars with dissimilar letters indicate significantly different values ($p < 0.05$). Each value is mean ± sd; n = 5.

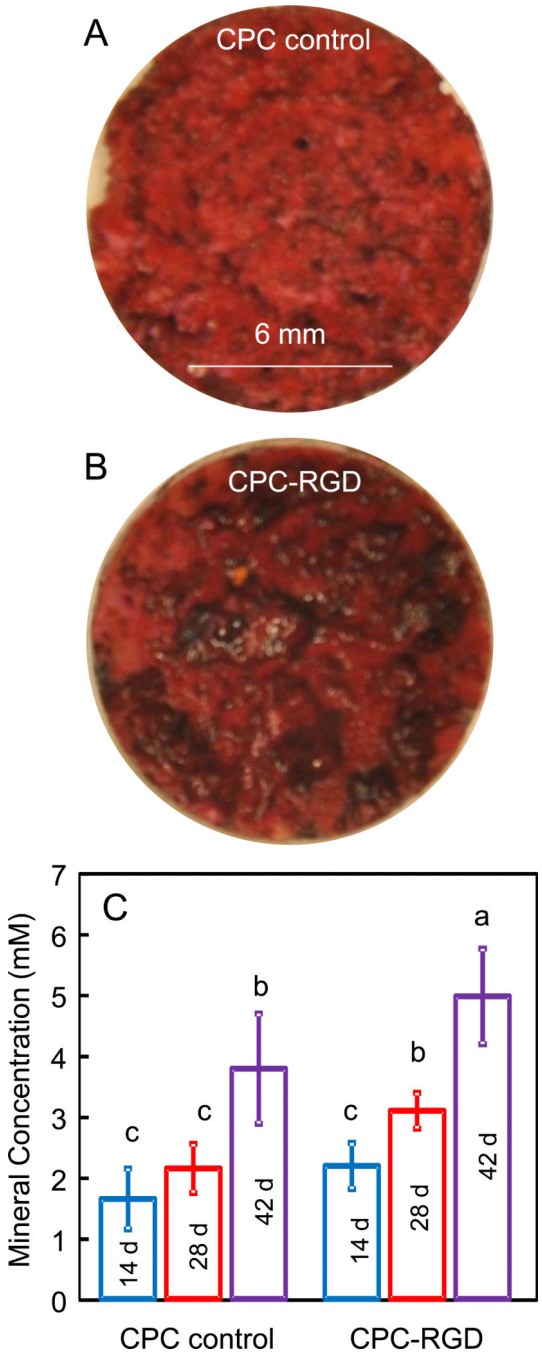

2.

Mineral synthesis by cells on CPC scaffolds. (A) ARS staining for CPC control. CPC disks were covered by a layer of new mineralized matrix synthesized by the cells (this example was for 42 d). (B) ARS staining for CPC-RGD at 42 d. CPC-RGD disks had a thicker layer of cell-synthesized matrix than CPC control. (C) Cell-synthesized mineral measured by the osteogenesis assay (mean ± sd; n = 5). Bars with dissimilar letters indicate significantly different values ($p < 0.05$). Mineral synthesis by HUVEC+HOB was greater on CPC-RGD than that on CPC control.

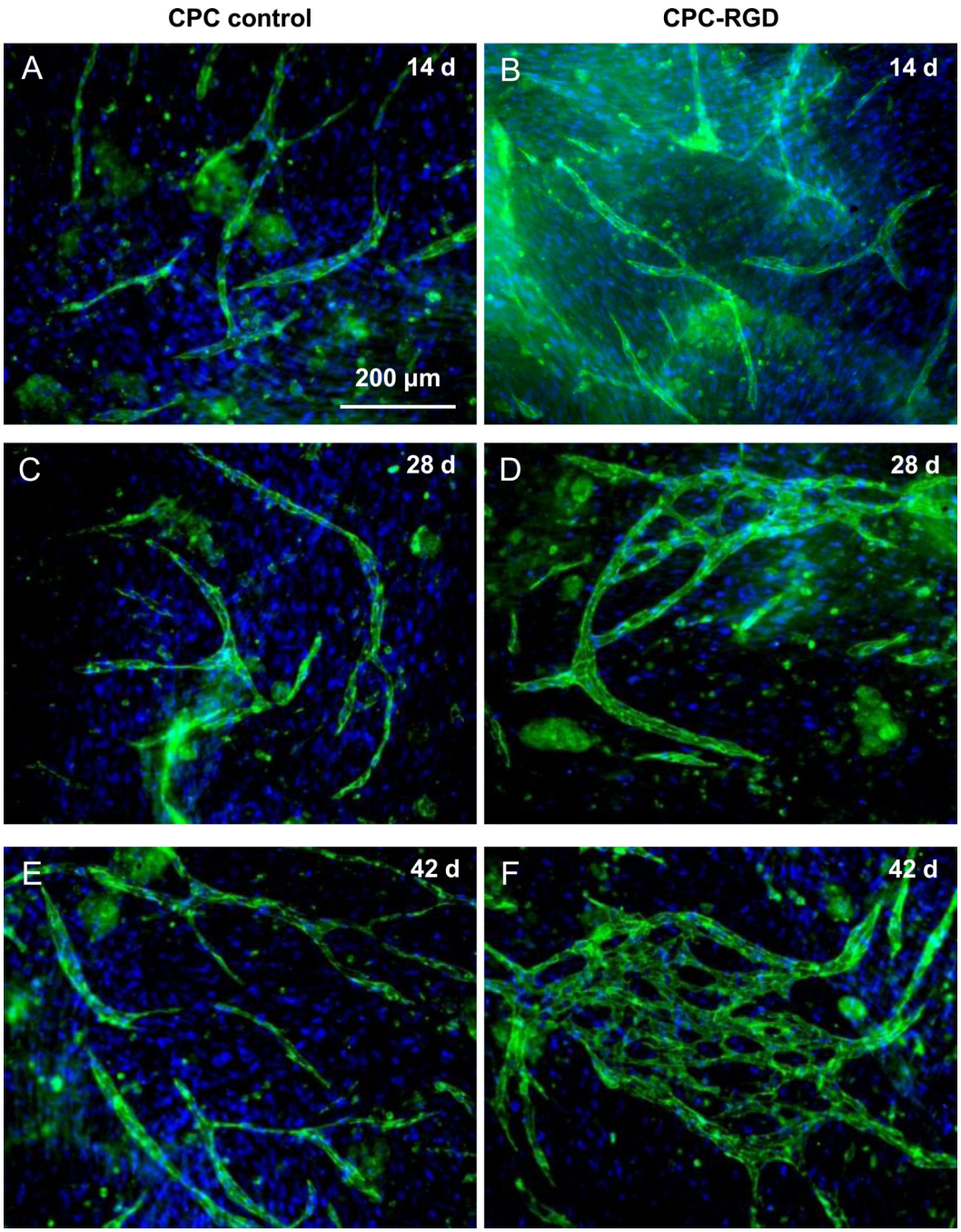

3.

Fluorescence images of HUVEC+HOB cocultured on macroporous CPC control and CPC-RGD scaffolds. HUVEC were identified by immunostaining with endothelial marker PECAM1 in green on the cell membrane, and the nuclei were counterstained with DAPI in blue. HOB were depicted by nuclei counterstaining with DAPI in blue but without green stain on the cell membrane. Microcapillary-like structures increased with culture time and with the incorporation of RGD in CPC.

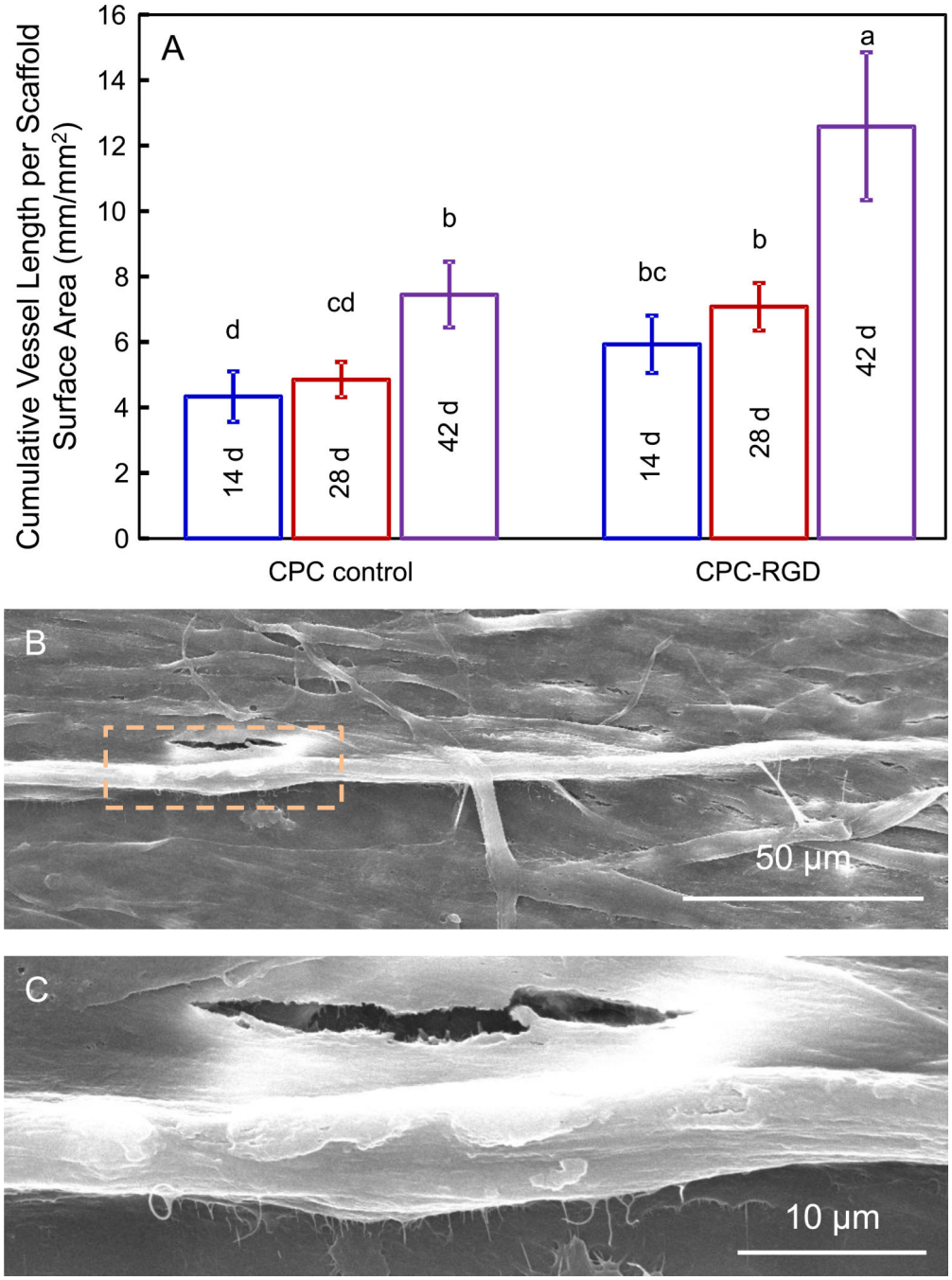

4.

Microcapillary-like structure formation on CPC scaffolds. (A) Cumulative length of microcapillary-like structures on CPC scaffolds. Bars with dissimilar letters indicate significantly different values ($p < 0.05$). The cumulative microcapillary lengths in images such as Fig. 3 were measured and divided by image area to yield the data in Fig. 4A (mean ± sd; n = 5). (B, C) Representative SEM images of microcapillary-like structures. These

images show examples of microcapillary structures on CPC-RGD at 14 d. Image C is a higher magnification of the square area in image B.